Developmental Cell
Article

# Functional Coupling between the Extracellular Matrix and Nuclear Lamina by Wnt Signaling in Progeria

Lidia Hernandez,[1,3,8] Kyle J. Roux,[4,8] Esther Sook Miin Wong,[5,8] Leslie C. Mounkes,[1] Rafidah Mutalif,[5] Raju Navasankari,[4,5] Bina Rai,[5] Simon Cool,[5] Jae-Wook Jeong,[6] Honghe Wang,[1] Hyun-Shik Lee,[2,9] Serguei Kozlov,[1] Martin Grunert,[5] Thomas Keeble,[5] C. Michael Jones,[5] Margarita D. Meta,[7] Stephen G. Young,[7] Ira O. Daar,[2] Brian Burke,[4] Alan O. Perantoni,[1] and Colin L. Stewart[1,5,*]
[1]Cancer and Developmental Biology Laboratory
[2]Laboratory of Cell and Developmental Signaling
NCI, Frederick, MD 21702, USA
[3]Molecular Signaling Section, Medical Oncology Branch, Center for Cancer Research, NCI, Bethesda, MD 20892, USA
[4]Department of Anatomy and Cell Biology, University of Florida College of Medicine, Gainesville, FL 32606, USA
[5]Institute of Medical Biology, Immunos, 8A Biomedical Grove, Singapore 138648
[6]Department of Molecular and Cellular Biology, Baylor College of Medicine, Houston, TX 77030, USA
[7]Department of Medicine, David Geffen School of Medicine, University of California, Los Angeles, CA 90095, USA
[8]These authors contributed equally to this work
[9]Present address: School of Life Sciences, College of Natural Sciences, Kyungpook National University, Daegu 702-701, South Korea
*Correspondence: colin.stewart@imb.a-star.edu.sg
DOI 10.1016/j.devcel.2010.08.013

## SUMMARY

**The segmental premature aging disease Hutchinson-Gilford Progeria (HGPS) is caused by a truncated and farnesylated form of Lamin A. In a mouse model for HGPS, a similar Lamin A variant causes the proliferative arrest and death of postnatal, but not embryonic, fibroblasts. Arrest is due to an inability to produce a functional extracellular matrix (ECM), because growth on normal ECM rescues proliferation. The defects are associated with inhibition of canonical Wnt signaling, due to reduced nuclear localization and transcriptional activity of Lef1, but not Tcf4, in both mouse and human progeric cells. Defective Wnt signaling, affecting ECM synthesis, may be critical to the etiology of HGPS because mice exhibit skeletal defects and apoptosis in major blood vessels proximal to the heart. These results establish a functional link between the nuclear envelope/lamina and the cell surface/ECM and may provide insights into the role of Wnt signaling and the ECM in aging.**

## INTRODUCTION

Aging is an inevitable consequence of life. With the identification of specific genes affecting longevity, considerable interest has arisen into understanding the molecular basis as to how organisms age (Friedman and Johnson, 1988; Kennedy et al., 1995). Among these genes is the mammalian Lamin A gene that encodes the A-type lamins, intermediate filament proteins that make up the bulk of the nuclear lamina (Gerace and Burke, 1988).

The A-type lamins have attracted much interest as at least eight diseases, the laminopathies, result from mutations within the *LMNA* gene (Burke and Stewart, 2006). Of these laminopathies, the most striking is the segmental premature aging disease Hutchinson-Gilford Progeria Syndrome (HGPS) (Gilford, 1904; Hutchinson, 1886). Newborns with HGPS are seemingly normal. By 12–18 months, they exhibit persistent growth retardation, hair loss, craniofacial abnormalities, osteolysis, and localized bone demineralization (Merideth et al., 2008). The children develop arteriosclerosis that is associated with loss of vascular smooth muscle cells, degenerative aortic weakness, and mitral valve disease. These conditions are inevitably fatal, due to stroke or myocardial ischemia during the child's mid-teens.

Lamin A protein undergoes posttranslational modification, involving transient farnesylation of the cysteine at the C-terminal CaaX motif, followed by removal of the farnesyl group and 18 amino acids by endoproteolytic cleavage by the protease ZMPSTE24/FACE1 (Corrigan et al., 2005). These modifications may be necessary for the localization of Lamin A protein to the nuclear envelope (Lutz et al., 1992). Defective posttranslational processing of Lamin A to its mature form results in about three-quarters of the HGPS cases (Csoka et al., 2004a; De Sandre-Giovannoli et al., 2003; Eriksson et al., 2003). The posttranslational defect is caused by a C-to-T nucleotide substitution at position 1824 in the *LMNA* gene that creates a premature splice donor site within exon 11. Inclusion of the novel splice donor site results in a 50 amino acid in-frame deletion within the C-terminal globular domain of Lamin A. The deletion eliminates the second endoproteolytic cleavage site, resulting in a truncated Lamin A protein (Progerin or LMNAΔ50) that remains farnesylated, and is incorporated into the nuclear periphery (Goldman et al., 2004).

Progerin results in abnormal nuclear morphologies, altered chromatin organization, delayed mitosis, lamina thickening, and growth arrest (Dechat et al., 2007; McClintock et al., 2006;

Scaffidi and Misteli, 2005). Short-term treatment of the cells with farnesyltransferase inhibitors (FTIs) rectifies the alterations in nuclear morphology and improves, to some extent, the viability of mouse lines retaining a farnesylated Lamin A protein (Capell et al., 2005; Glynn and Glover, 2005). Whether all these pathological effects are solely due to persistent farnesylation or are compounded by the deletion of the 50 amino acids is unclear (Yang et al., 2008). Intriguingly, evidence has emerged suggesting low levels of progerin may be expressed in fibroblasts from old individuals and in late passage normal cells (McClintock et al., 2007; Rodriguez et al., 2009; Scaffidi and Misteli, 2006). How progerin causes HGPS and whether it contributes to the "normal" aging process is an area of intensive speculation.

Previously we described a mouse line carrying a mutated *Lmna* gene (*Lmna*$^{L530P/L530P}$, herein called Δ9*Lmna*) that develops many of the pathologies associated with HGPS, including craniofacial, dental, and skeletal abnormalities, loss of subcutaneous fat, diminished postnatal growth, and early death (Mounkes et al., 2003). The mutation results in the deletion of exon 9 producing a truncated form of lamin A that we here show remains farnesylated, demonstrating that this mouse line provides a model to uncover the molecular etiology and pathology of HGPS, which we here describe.

## RESULTS

### The *Lmna* Δ9 Mutation Results in a Truncated yet Farnesylated Form of Lamin A

The *Lmna*Δ9 mutation in our progeric mouse model causes skipping of exon 9, resulting in an in-frame deletion of 40 amino acids from the Ig fold in the C-terminal globular domain of the lamin A and C proteins. This results in an overall reduction of *Lmna* transcript levels and protein (Mounkes et al., 2003).

The consequences of the Δ9 deletion on the processing and nuclear localization of lamin A protein were examined using an HA-tagged LMNA-WT C-terminal globular domain (WT tail) and HA-tagged LMNAΔ9 tail domain expressed in HeLa cells. Human *LMNA* cDNA constructs were used as the mouse and human *LMNA* genes show 98% homology. Restricting the use to the tail domain overcomes potential complications arising from interactions between the mutant and full-length A-type lamins in analyzing defects in posttranslational processing (Hennekes and Nigg, 1994). The transfected cells were lysed in TX-114 buffer and the phases separated. The majority of the slower-migrating LMNA-WT tail was detected in the aqueous (Aq), but not detergent phase (TX-114). Prelamin A (arrow) was distinct from the mature lamin A (arrowhead). The LMNAΔ9 variant was detected as a single band (*) present in both the aqueous and detergent phases, indicating that LMNAΔ9 does not undergo efficient cleavage and about 50% of the protein partitions to the detergent phase presumably due to the mature form remaining farnesylated (Figure 1A).

We next examined whether LMNAΔ9 is farnesylated. In this context, the CSIM variant refers to a wild-type CaaX motif in normal prelamin A; in the SSIM variant, this cysteine is replaced with a serine residue that cannot be farnesylated. HA-tagged full-length CSIM and SSIM variants of the WT-LMNA and LMNAΔ9 were translated in reticulocyte lysates in the presence of either $^{35}$S-labeled cysteine and methionine or $^{3}$H-labeled mevalonolactone (a precursor for farnesyl moieties). Autoradiographs of the separated proteins reveal similar levels of protein translation as observed by $^{35}$S labeling (Figure 1B, upper panel). Incorporation of $^{3}$H-mevalonolactone into the lysates showed the CSIM and not the SSIM variants were farnesylated (Figure 1B, lower panel). To confirm this, HA-tagged full-length WT-LMNA and LMNAΔ9 were translated together with 20 μM of the farnesyltransferase inhibitor (FTI) PB-43. In the presence of the FTI the $^{3}$H farnesyl moiety was not incorporated in any of the lamins (Figure 1C).

A key issue in progeria is that proteolytic removal of the farnesyl group is impaired. To determine if the LMNAΔ9 variant was processed following farnesylation, HA- or MYC-tagged CSIM or SSIM amino acid variants of full-length WT-LMNA and LMNAΔ9 were separated by SDS-PAGE and immunoblotted with anti-HA, MYC or prelamin A antibodies (Figure 1D). As detected with anti-epitope tag antibodies (top panel) the LMNAΔ9-CSIM remains similar in size to the SSIM variant, unlike the WT-LMNA which is processed to mature lamin A, which migrates faster than the SSIM variant. This was confirmed by immunoblotting with prelamin A-specific antibodies detecting significant amounts of all lamin variants, except the predominantly processed WT-LMNA-CSIM (lower panel). LMNAΔ9 is therefore not efficiently cleaved into a mature form.

Last, we determined if LMNAΔ9 is targeted to the nuclear envelope (NE). HA- or MYC- tagged full-length CSIM and SSIM variants of WT-LMNA or LMNAΔ9 were transfected into *Lmna* null MEFs and their localization assessed by immunofluorescence. The CSIM variant of LMNA-WT was predominantly detected at the nuclear envelope, whereas the unfarnesylated SSIM WT-LMNA was largely nucleoplasmic. Similar results were observed for LMNAΔ9. Despite a lack of cleavage, LMNAΔ9-CSIM is similar to farnesylated lamin A as it localizes to the NE (Figure 1E).

### LmnaΔ9 Inhibits Postnatal, but Not Embryonic, Fibroblast Proliferation

HGPS children are seemingly normal at birth, with the first signs of the disease appearing at 6–18 months. The delayed manifestation of the disease is reflected by the proliferative characteristics of progeric fibroblasts, in that they initially proliferate normally and then sometimes undergo a rapid decline in proliferative capacity (Bridger and Kill, 2004). Similarly, the Δ9 mice are also overtly normal at birth, with weights identical to those of their heterozygous and wild-type siblings. However, the homozygotes show growth retardation within the first week (Mounkes et al., 2003).

We investigated if proliferation of LMNAΔ9-expressing embryonic fibroblasts (MEFs) from E13 embryos was affected. Both short-term and long-term (3T3) proliferation assays revealed the Δ9MEFs proliferated at rates almost identical to those of +/+MEFs, with only a slight reduction in total cell number being observed in the long-term cultures (Figure 2A). This was surprising as nuclear morphologies of the Δ9MEFs were abnormal (Figure 2A, insert).

We then analyzed the growth of Δ9 postnatal fibroblasts (MAFs), using primary fibroblast lines established from kidney, skin, lung and skeletal muscle, of 2- to 3-week-old mice to determine if there was any topographical variation in proliferation (Chang et al., 2002). In contrast to the Δ9MEFs, Δ9MAFs from

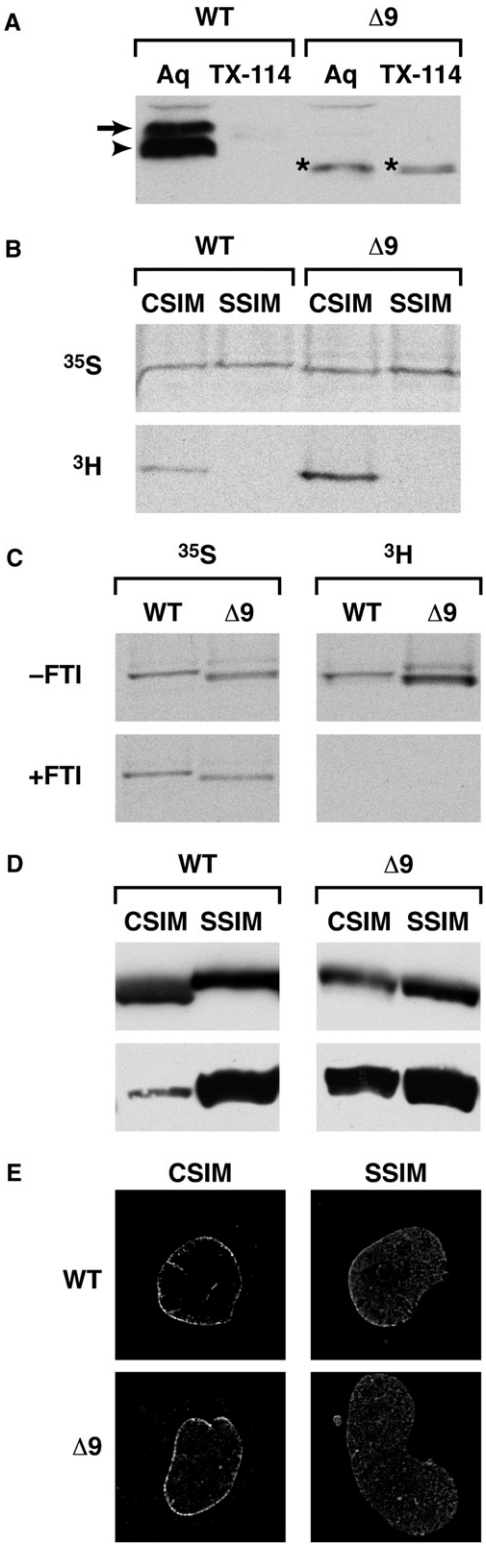


**Figure 1. Δ9LaminA Is Farnesylated and Not Processed to a Mature Form**

(A) WT LMNA tail partitions to the aqueous phase (Aq), not the detergent phase (TX-114). PrelaminA (arrow) is distinct from mature LMNA (arrowhead). The LMNAΔ9 tail is a single band (*) and partitions to both aqueous and detergent phases.

(B and C) HA-tagged full-length CSIM and SSIM variants of LMNA WT and Δ9 were translated with $^{35}$S-labeled cysteine and methionine or $^{3}$H-labeled-mevalonolactone in the presence (C) or absence of 20 μM farnesyltransferase inhibitor PB-43.

(D) HA- or myc-tagged CSIM or SSIM variants of full-length human LMNA-WT and Δ9 were immunoblotted with anti-HA or Myc (top panel) or prelamin A antibodies (lower panels). LMNAΔ9-CSIM is similar in size to the SSIM variant (top right panel). CSIM WT-LMNA is processed and migrates faster than the SSIM variant (top left panel).

(E) NE versus nucleoplasmic localization of CSIM and SSIM variants of LMNA-WT and Δ9 was analyzed by immunofluorescence in *Lmna*$^{-/-}$ MEFs.

all tissues showed accelerated senescence and death (Figure 2B) even though Δ9MEFs and MAFs expressed LMNAΔ9 at the same levels (see Figure S1 available online). Around p4-5 the Δ9MAFs started to detach from the dish (Figure 2C, right panel) as they underwent apoptosis at twice the level (~7%) of wild-type MAFs (Figure 2D).

To verify the effect of the Δ9 mutation on cell proliferation and to compare Δ9 with Progerin (Δ50), we introduced each mutant form of *LMNA*, into primary *Lmna* null MAFs by retroviral vector-mediated infection (Figure 2E) that resulted in equivalent levels of expression of the different variants in the infected cells (Figure 2F). *Lmna*$^{-/-}$ MAFs show accelerated entry into senescence, followed by the emergence of derivatives with enhanced proliferative capability (Figure 2H). With the stable incorporation of Lamin A into the lamina of *Lmna*$^{-/-}$ MAFs, a regular nuclear morphology is restored, (Figure 2G3) and the cells become senescent, typical of wild-type cells (Figure 2H). In contrast, both Δ9 and Δ50, both of which were incorporated into the lamina, resulted in abnormal nuclear morphologies and blebbing (Figures 2G1 and 2G2, respectively). Both mutant forms resulted in identical rates of accelerated proliferative arrest compared to cells expressing WT-Lamin A (Figure 2H).

### *Lmna*Δ9 MAFs and Skeleton Show Altered Expression of Extracellular Matrix and Cell Adhesion Genes

A possible cause of the inability of Δ9MAFs to proliferate and their rapid death may have been genomic instability, because human progeric lines show increased frequencies of chromosome breakage and defective DNA repair, particularly at telomeres (Liu et al., 2006). We were unable to find any evidence for increased mitotic recombination, aneuploidy, chromosomal breakage, or failure in DNA repair mechanisms as measured by H2AX staining following UV irradiation in the Δ9MAFs (data not shown). Telomerase activity was also unaffected (data not shown). We therefore performed an Affymetrix microarray-based gene expression analysis of passage 3 Δ9 and +/+MAFs from 2- to 3-week-old siblings. Data were analyzed using the Robust Multichip Algorithm (RMA) (Irizarry et al., 2003). Significant changes in the expression of 194 transcripts, encoding 170 annotated genes (Table S1 available online; Figures S2A and S2B) were identified (false discovery rate <0.001; fold change >1.5). GO analysis of the transcript list, using the DAVID bioinformatics resource (Thomas et al., 2003), revealed the most significant molecular function grouping was for extracellular matrix ($p < 3.9E^{-10}$) (Tables S2A and S2B). We verified these results by relative quantitation (RQ) PCR analysis on a subset of 12 of the ECM/cell adhesion genes (Table S2B), confirming

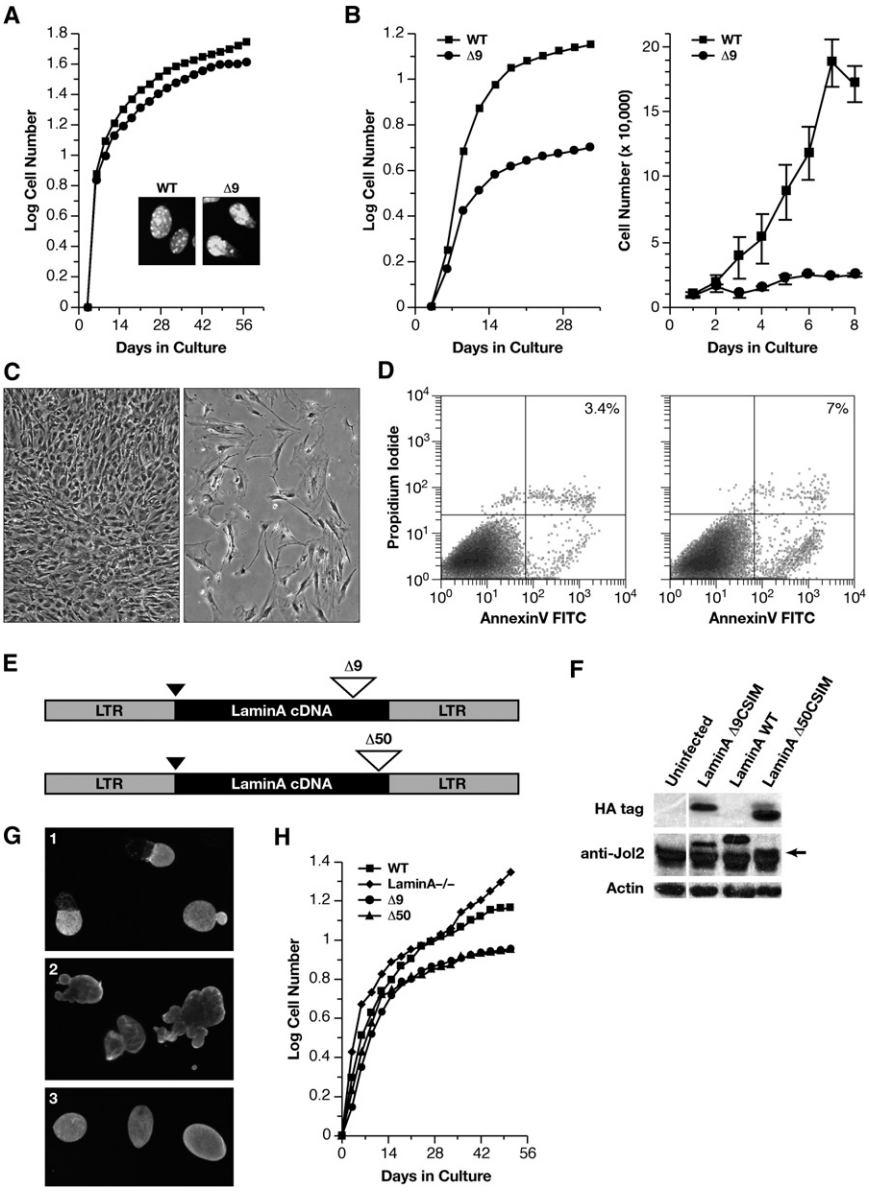


**Figure 2. Δ9 and Δ50 Result in Abnormal Nuclear Morphologies and Accelerated Proliferative Arrest**

(A) WT (■) and Δ9 (●) MEF growth curves, with nuclear morphology shown in the insets (DAPI staining).

(B) WT (■) and Δ9 (●) MAF growth curves.

(C and D) Passage 4-5 WT (left panels) and Δ9 (right panels) MAFs assayed for morphology (C) and apoptosis (D).

(E) Retroviral vectors for Δ9 or Δ50 HA-tagged LMNA cDNAs. HA tag (black triangle) and deletions (open triangles).

(F) Western analysis of retroviral protein production. WT-LMNA is not HA tagged; all Lamins are detected by the Jol2 monoclonal antibody specific for hLMNA. The Δ50hLMNA band (arrow) migrates just above a nonspecific band detected in all samples by Jol2.

(G) Jol-2 immunostaining reveals nuclear morphology in cells expressing Progerin/Δ50 (G1), Δ9 (G2), and Wt Lmna (G3).

(H) *Lmna*$^{-/-}$ cells proliferate and immortalize. Growth curves show the effect of reintroduction of LMNA constructs.

significantly reduced expression in the Δ9MAFs (Figure 3A). In contrast, Δ9MEFs and +/+MEFs showed only minor differences in gene expression (Figure 3A).

Many of the ECM genes, with reduced expression, are components of the cartilaginous and boney skeleton. Gene expression comparisons from age-matched Wt and Δ9 mice in the calvaria, tibias, and femurs revealed the majority of the same ECM genes were significantly reduced in Δ9 skeletal tissues (Figure 3A).

GO analysis of biological processes revealed that mesonephros, skeletal development, and cell adhesion were significantly represented (Table S2C). We did not detect any pathology associated with the kidneys; however, the skeletal system showed reduced mineralization (Mounkes et al., 2003). A high-resolution microCT comparison of skeletons of 2- to 3-week-old Δ9 age-matched with Wt siblings (three of each genotype) revealed the mutants have reduced density in the calvaria and long bones (Figures 3B and 3C, respectively). Bone volume to total volume ratio were significantly reduced in the tibias and femurs ($p < 0.04/0.01$) of the Δ9mice, as were trabecular thicknesses and number in the tibias and femurs $p < 0.001/0.04$, respectively) (Figure 3D). Calvarial, as well as tibial and femoral stiffness were reduced, shorter tibial tuberosity, evidence of rib fractures, were also detected, all of which indicated increased bone fragility.

A histopathological analysis and TRAP staining for endosteal and periosteal osteoclasts in the femurs and skulls revealed no overt differences in cellular organization or numbers of osteoclasts between the wild-type and Δ9 skeletal systems (data not shown) indicating that the reduction in bone density was not associated with increased osteoclast numbers.

## Vascular Smooth Muscle of the Great Vessels Is Thinner and Exhibits Extensive Apoptosis

The early to mid-teen death of progeric patients is due to cardiovascular defects resulting in a heart attack or stroke. A feature of the pathology is loss of vascular smooth muscle cells (VSMC) in the aorta, and other great vessels (Stehbens et al., 2001). Histological examination of the hearts and great vessels revealed that the VSMC layer in the pulmonary artery showed thinning in six homozygous Δ9 mice compared with age-matched (2) +/+ and (4) +/− siblings at 2 weeks after birth. TUNEL analysis revealed extensive apoptosis throughout the circumference of the VSMC layer of the artery (Figure 3E). Only a few apoptotic cells

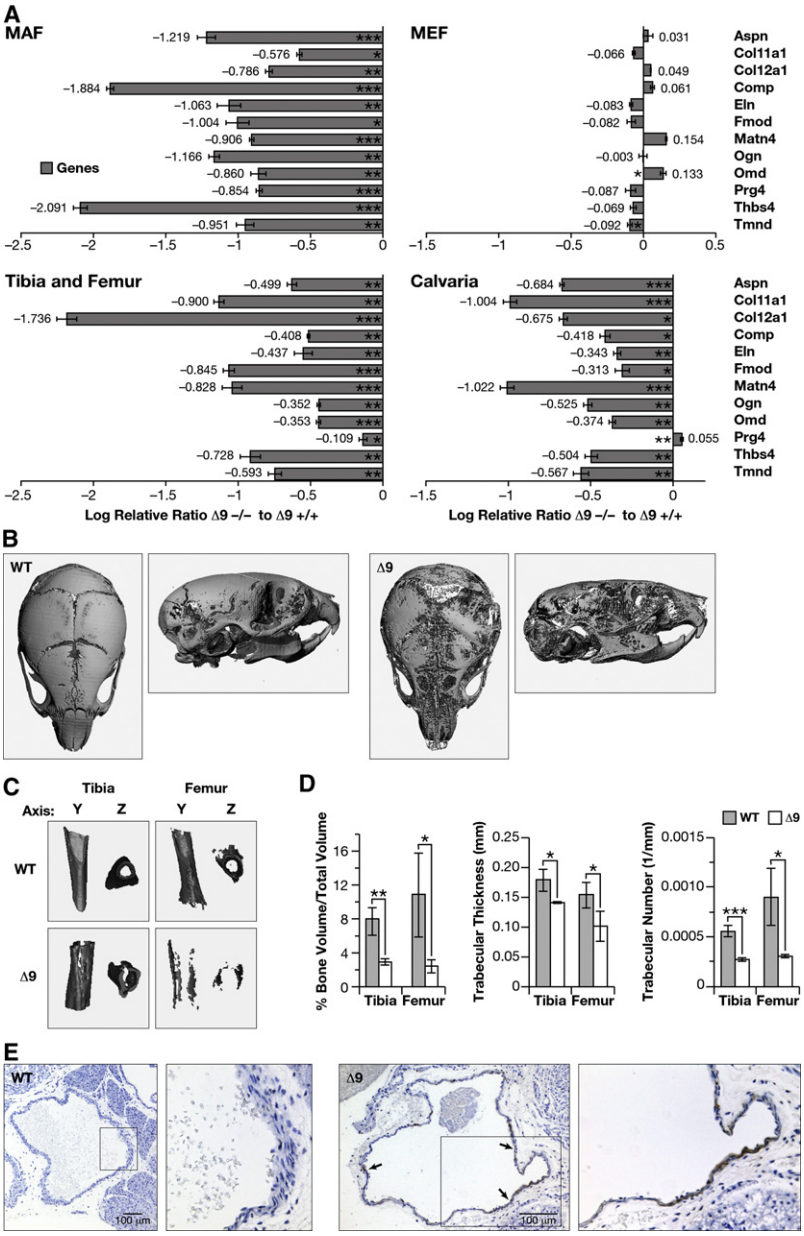


**Figure 3. Δ9 Mice Show Reduced ECM Gene Expression and Abnormal Skeletal and Vascular Development**

(A) Confirmation of the microarray analysis (Tables S1 and S2A–S2C and Figures S2A and S2B) by RQ-PCR. Differences are expressed as the relative log ratio between the Δ9 and Wt samples, with a 2-fold decrease being equivalent to −0.301, 4-fold decrease −0.602, 5-fold decrease −0.699, *p < 0.05, **p < 0.01, and ***p < 0.005 at the 95% confidence interval. Error bars are SEM.

(B–D) Calvarial (B) and long bone (C) mineral density, as well as long bone volume and trabecular thickness and number (D) in P14 WT and Δ9 sibling mice; *p < 0.05, **p < 0.01, and ***p < 0.005 (three of each genotype).

(E) Apoptosis in pulmonary artery smooth muscle of P16 WT and Δ9 mice (TUNEL staining indicated by arrows).

were detected in the ventricles and other regions of the heart (data not shown).

## Defective ECM Synthesis Results in Proliferative Arrest and Is Not Rescued by FTI Treatment

To determine if the reduction in ECM protein expression resulted in proliferative arrest and apoptosis of Δ9MAFs, we cultured Δ9MAFs under continuous proliferation conditions on dishes precoated with ECM deposited by wild-type fibroblasts. Precoated dishes were prepared by culturing wild-type MAFs to confluency and maintaining them for a week under contact-mediated growth arrest. Under these conditions, the cells deposit an ECM that remains on the dish after gentle lysis and removal of the cells (Gospodarowicz et al., 1980). The results reveal that Δ9MAFs consistently grew to passages comparable to wild-type cells when maintained on the ECM derived from +/+MAFs (Figure 4A). On wild-type ECM, Δ9MAFs attained a higher cell density with fewer detached cells (Figure 4B, right panel). We also cultured the cells on dishes pretreated with fibronectin, collagen, laminin, or thrombospondin, all which showed reduced expression in the array data. None of these factors (including matrigel) were effective at rescuing the proliferative failure of the Δ9MAFs, although improved growth rates were noted with all except fibronectin, with thrombospondin being the most effective (Figure S3A), suggesting that a combination of ECM factors is required for MAF proliferation.

The farnesyl transferase inhibitor PB-43 improves the nuclear shapes of progeroid mice and human fibroblasts in short term culture (Toth et al., 2005). Treatment of the Δ9MAFs with PB-43 did not rescue their proliferation at different concentrations (100 nm to 5 μm). In fact growth of the Δ9, as well as +/+ MAFs, was severely inhibited by the FTI (Figure S3B). We also observed similar negative effects on +/+ and Δ9MAF proliferation by two other FTIs, FTI-277 and FTI-276 (Calbiochem), at 1 and 3 μM concentrations (data not shown).

## Canonical Wnt Signaling Is Inhibited by Δ9 and Δ50 *LMNAs*

To understand how a mutation in nuclear Lamin A results in significant changes in the ECM, we analyzed which signaling pathways were potentially affected. Analysis of the array data revealed that components of Tgf-β superfamily (Bmp4 and 5, Smad6, Ltbp-3), Wnt family (Ftz8, R-spondin, Dapper), and Notch (notch3) signaling pathways were altered in their expression.

Treatment of the Δ9MAFs with either Bmp4 or 5 only slightly improved MAF viability and proliferation (data not shown).

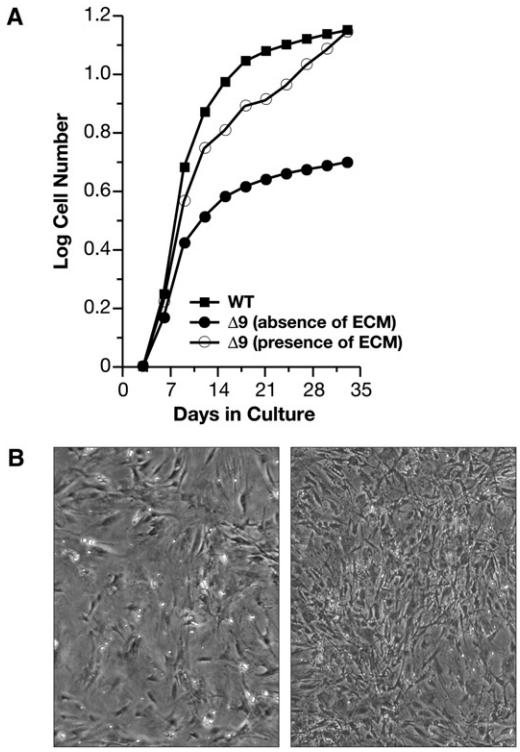


**Figure 4. Δ9MAF Growth Is Rescued by WT Extracellular Matrix**

(A) Growth curves of WT MAFs and of Δ9MAFs in the presence or absence of WT MAF ECM.

(B) Left panel Δ9MAFS at p4 with no ECM; right panel Δ9MAFs on ECM. Growth of Δ9MAFs on specific ECM components or with FTIs is shown in Figures S3A and S3B.

To determine if the Δ9 and Δ50 lamins affected the canonical Wnt signaling pathway, we performed TOPFlash luciferase reporter assays for β-catenin-mediated transcriptional activity (Morin et al., 1997). Plasmids containing cDNAs of wild-type *LMNA*, *LMNAΔ9*, *LMNAΔ50*, their respective SSIM variants, as well as native β-catenin and luciferase reporter vectors were transfected into HEK293 cells with equivalent amounts of DNA for each transfection (Yin et al., 2005). LMNAΔ9 significantly inhibited β-catenin-mediated Lef1-regulated transcription by approximately 85% and LMNAΔ50 also inhibited β-catenin activity, but to a lesser degree (50%) than Δ9, while the SSIM version of LMNAΔ9 was only mildly inhibitory and the SSIM version of LMNAΔ50 had no effect (Figure 5A).

We investigated whether the abundance of the β-catenin form that preferentially binds to Lef1transcription factors was reduced in HEK293 cells expressing LMNAΔ9 using a semiquantitative specific TCF-GST pull-down assay (Gottardi and Gumbiner, 2004). LMNAΔ9-expressing cells showed a 70% reduction in the nuclear levels of Lef1-binding to β-catenin compared with controls, indicating that Δ9 reduced the levels of active Tcf/Lef-β-catenin. LMNAΔ50, SSIM, and the +/+ forms had milder inhibitory effects, suggesting that the deletions, as well as the farnesylated status of the lamins contribute to the effect on Wnt signaling (Figure 5B). Immunohistochemical staining of the *Δ*9MAFs, +/+ cells and *LMNAΔ9* transfected cells did not reveal any obvious differences in β-catenin nuclear localization between the +/+ and mutant cells (data not shown).

## Wnt, but Neither Tgf-β/nodal nor Notch Signaling, Is Inhibited by LMNAΔ9in *Xenopus* Embryos

Injection of two- to four-cell stage *Xenopus* embryos with either Xwnt3a or Xwnt8 mRNA results in the dorsalization and axis duplication during larval stages. Xwnt3a mRNA alone or with *LMNA*-WT mRNA resulted in approximately 75% of the larvae becoming dorsalized and/or developing a duplicated axis, with no larvae showing normal development (Figure 5C). In contrast, coinjection with *LMNAΔ9* mRNA suppressed Xwnt3a-mediated duplication, resulting in only 25% of the larvae dorsalizing, with 50% of the larvae developing normally. Coinjection of the unfarnesylated *LMNAΔ9-SSIM* mRNA variant had no inhibitory effect on axis duplication and dorsalization. *LMNAΔ50* variants only marginally inhibited axis duplication. Similar results were obtained using Xwnt8 mRNA (data not shown).

We analyzed whether other signaling pathways, including the Tgf-β/Nodal and Notch pathways were influenced by *LMNAΔ9* mutation, as progerin may activate the Notch signaling pathway in human mesenchymal stem cells (Scaffidi and Misteli, 2008). Injection of Nodal mRNA into both ventral blastomeres at the four-cell stage results in dorsalization of ventral explants (Jones et al., 1995). This phenotype was not inhibited by coinjection of the *LMNAΔ9* mRNA (93 embryos tested). Similarly, injection of the *LMNAΔ9* mRNA into a two-cell stage blastomere did not affect Notch-mediated effects on neurogenesis (49 embryos tested) (Vernon et al., 2006).

## Impaired Wnt Signaling Is Due to Reduced Nuclear Levels and Transcriptional Activity of Tcf/Lef1

Analysis of the differentially expressed genes in the Δ9MAFs revealed that at least four—fibronectin, Bmp4, Col11A1, R-spondin—are trancriptionally regulated by the Wnt pathway. We focused on Col11A1 as the binding sites of the canonically regulated transcription factor Lef1 were mapped to the promoter region of the mouse Col11A1gene (Kahler et al., 2008). ChIP analysis, using chromatin isolated from +/+MAFs confirmed the binding to a region −541 to +269 around the transcriptional start site. Binding of Lef1 to this region was reduced by 60% in Δ9MAFs, and was enhanced by pretreatment of the cells with the Gsk-3β inhibitor SB415286 (Figure 6A; Coghlan et al., 2000). The reduction in Lef1 binding to the promoter was due to a marked reduction (>90%) in Lef1 levels in the Δ9MAFs (Figure 6B), as measured by RT-PCR and was confirmed by western analysis on nuclear extracts and immunofluorescence, revealing reduced accumulation of Lef1 in the Δ9 nuclei (Figures 6C and 6D). This was specific for Lef1, as Tcf4 expression was unaffected (Figures 6C and 6D). Significantly Lef1 is not detectable in +/+MEFs, whereas Tcf4 is expressed (Figure 6C), revealing a difference in Lef1 expression between +/+MEFs and MAFs. A comparison of two human progeric fibroblast lines (AG11498, AG06297) with a fibroblast line from a normal parent (AG03512), by western analysis of nuclear extracts and immunofluorescence revealed that nuclear expression of LEF1, but not TCF3/4, was also markedly reduced in the progeric fibroblasts compared with normal fibroblasts (Figures 6E and 6F).

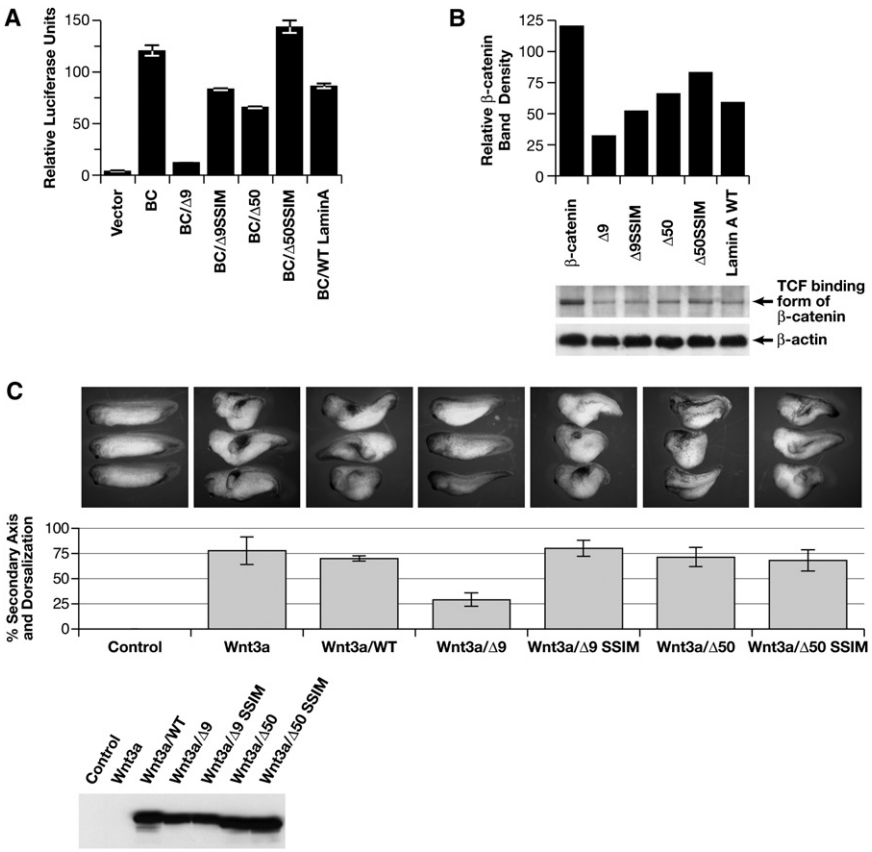


**Figure 5. Δ9 and Δ50 Lamin Inhibit Wnt-Mediated Transcription**

(A) TOPflash/FOPflash luciferase reporter assays with WT (BC), Δ9, Δ50 lamins, or their SSIM variants.

(B) Gst-Tcf pull-down of nuclear β-catenin levels.

(C) Injection of Xwnt3a mRNA into Xenopus embryos, alone or in the presence of each LMNA construct shown in (A) and (B). Lower panel, western analysis shows amount of protein derived from the different *LMNA* mRNAs injected. Error bars are SEM.

conformation of the Ig fold and hence the overall structure of the C-terminal globular domain. Disruption to the domain may therefore prevent the endoprotease, Zmpste24, recognizing the second endoproteolytic site and efficiently processing the removal of the farnesylated peptide. Our mouse model is therefore a valid resource to determining the pathological consequences of a persistently farnesylated, truncated Lamin A protein.

In many of the laminopathies the pathology does not manifest until well after birth, despite A-type lamins being robustly expressed during embryogenesis (Rober et al., 1989; Stewart and Burke, 1987). HGPS newborns are seemingly normal with the first clinical symptoms, becoming apparent at 6–12 months (Merideth et al., 2008). We noted that Δ9 newborn mice are normal with growth retardation commencing during the first week and death ensuing at 3–4 weeks (Mounkes et al., 2003). In line with these effects on in vivo growth, we find that Δ9MAF proliferation ceases, with progerin also inhibiting MAF proliferation. In contrast, Δ9MEFs, expressing identical LaminA levels, are unaffected, consistent with normal fetal development. Although the Δ9MEFs have abnormal nuclear morphologies, we were unable to detect any significant differences in proliferation or gene expression (apart from slightly altered levels in oncomodulin and tenomodulin) between Δ9 and +/+MEFs. Fibroblast proliferation, with respect to the Δ9mutation, is therefore profoundly influenced by whether the cells are of embryonic or postnatal origin.

As we found no evidence of gross genome instability (Dechat et al., 2007; Liu et al., 2005) associated with the proliferative decline in the Δ9MAFs (data not shown), we focused instead on a defective ECM as the basis for impaired MAF proliferation, consistent with previous reports, where ECM components were the second largest group of genes misregulated in cultured HGPS cells (Csoka et al., 2004b). A defective ECM is specific to the Δ9mutation and not a consequence of reduced levels of A-type lamins, as array analysis of *Lmna* null MAFs (Sullivan et al., 1999) shows no significant alterations in the expression of ECM genes (data not shown).

### Rescue of *Lmna*Δ9 and Human Progeric Cell Proliferation by Inhibition of Gsk-3

Gsk-3α and β regulate the canonical Wnt signaling pathway by phosphorylating and promoting the degradation of β-catenin. Inhibition of Gsk-3β stabilizes β-catenin levels, resulting in enhanced β-catenin-mediated transcriptional activity (Behrens et al., 1996). We treated *Δ9* and +/+MAFs with recombinant Wnt3a protein or Wnt conditioned media but this did not improve cell viability or proliferation. However, treatment with the SB415286 inhibitor was effective. Inhibitor treatment stimulated proliferation and viability of the Δ9MAFs in a dose responsive manner, with 25 μM being the most effective at restoring the survival and proliferation of the Δ9MAFs to a level comparable to that of normal MAFs (Figure 7A), whereas the +/+MAFs were only marginally stimulated by the inhibitor. At a dose of 10 μM, SB-415286 also significantly improved proliferation of the human progeric line AG06297 (Figure 7B).

## DISCUSSION

Hutchinson-Gilford Progeria is caused by mutations in the *LMNA* gene. Here, we have characterized the molecular and cellular changes associated with the pathology of our previously reported mouse model for HGPS (Mounkes et al., 2003). The *Δ9* mutation results in the in-frame deletion of 40 amino acids from the Ig fold domain of Lamin A. LaminAΔ9 protein remains farnesylated, presumably because the deletion affects the

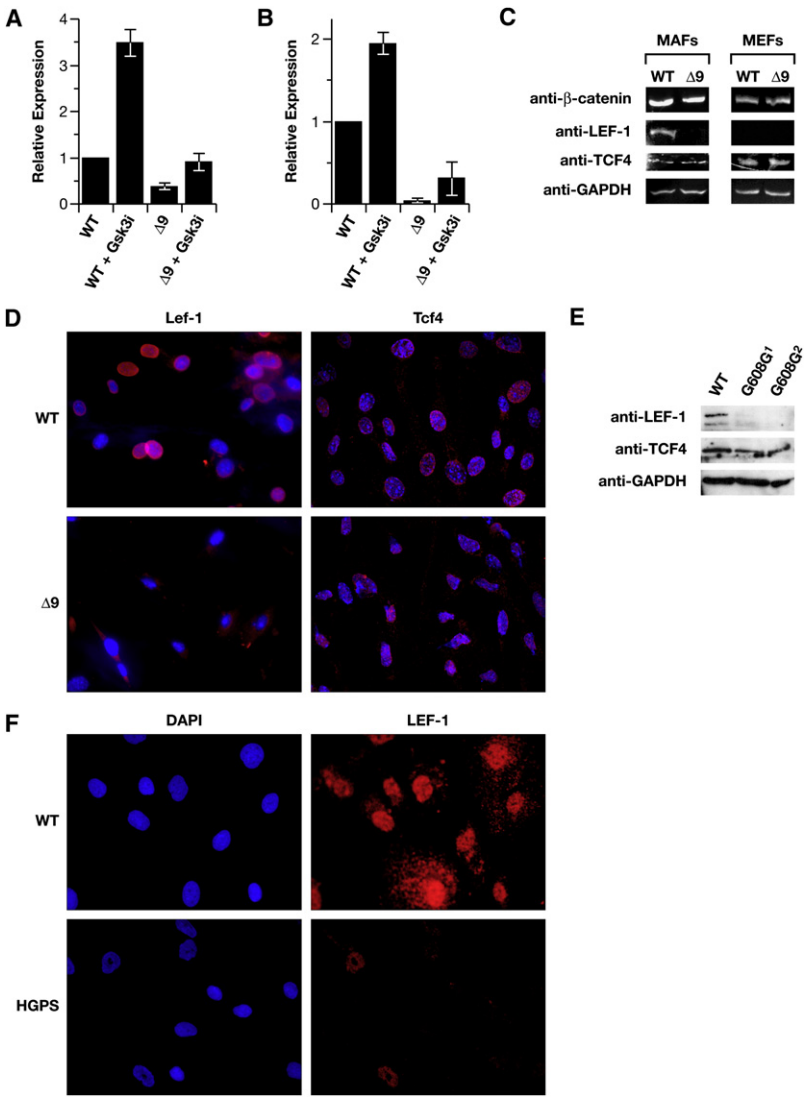


**Figure 6. Lef1 Levels Are Reduced in Δ9 and Progeric Cells**

(A) ChIP analysis of Lef1 binding to the *Col11A1* promoter in WT and Δ9 MAFs, in the presence an absence of pretreatment with the SB415286 Gsk-3β inhibitor (10 μm).

(B) RT-PCR detection of Lef1 mRNA in WT and Δ9MAFs.

(C) Western analysis of β-catenin, Lef1, and Tcf4 in WT and Δ9MAFs and MEFs.

(D) Immunofluorescent detection of Lef1 and Tcf4 in WT and Δ9MAF nuclei counterstained with DAPI.

(E) Lef1 and Tcf4 detection by Western analysis of nuclear extracts of fibroblast lines from two progeric patients (Coriell #AG11498, AG06297).

(F) Immunofluorescence showing Lef1 in normal parental (WT- AG03512) and progeric (AG11498) fibroblasts, nuclei counterstained with DAPI.

Error bars are SEM.

Why, during the transition from embryonic to postnatal stages, Δ9 fibroblast proliferation becomes dependent on an ECM is unclear. One possibility is that changes in proliferation reflect and depend on different functions (and composition) of the ECM between embryogenesis and postnatal life. During embryogenesis, the ECM regulates cell migration, adhesion, differentiation, and morphogenesis (Adams and Watt, 1993). Postnatally, the ECM assumes a more structural role in maintaining tissue integrity and homeostasis, particularly in tissues subjected to extensive mechanical stress such as the skeletal and cardiovascular systems (Brooke et al., 2003; Kjaer, 2004). In fibroblasts, ECM composition and integrin expression changes both qualitatively and quantitatively during the transition from embryonic to postnatal life (Chang et al., 2002). These changes have functional consequences, as fetal and adult fibroblasts differ in their adhesive and migratory parameters, and in their responses to growth factors (Brink et al., 2005; Ellis and Schor, 1996).

The differences in MAF gene expression are reflected by similar reductions for the same genes in the Δ9 skeletons. These declines may underlie the skeletal pathologies associated with HGPS and are consistent with skeletal abnormalities in other mouse models for progeria (Bergo et al., 2002; Varela et al., 2005). Expression of many small leucine-rich repeat glycoproteins (SLRPs), including COMP, osteoglycin, osteomodulin, PRELP, and fibromodulin, was reduced. Collagen fibril assembly depends on these SLRPs, as well as collagen XI (Kadler et al., 2008), which was also reduced in the Δ9MAFs. Defective synthesis of these proteins results in osteoporesis, osteoarthritis, and muscular dystrophy (Ameye and Young, 2002; Aszodi et al., 2006). Intriguingly, the progeroid variant of Ehlers-Danlos syndrome (OMIM 130070), that shares some of the pathologies found in HGPS, such as short stature, osteopenia, skin defects, and hair loss, is caused by defects in galactosyltransferase I, an enzyme essential for proteoglycan synthesis; mice doubly deficient in the SLRPs, Decorin, and Biglycan also mimic this phenotype (Corsi et al., 2002). ECM anomalies may also underlie the increase in apoptosis in the VSMC in some of the great vessels around the heart. Autopsies on HGPS patients noted the marked loss of smooth muscle in the aortas and arteries that is associated with disorganization of the surrounding ECM, collagen fibrils, and basement membranes (Stehbens et al., 2001), structures whose composition changes significantly postnatally and are essential to maintaining vascular integrity (Wagenseil and Mecham, 2009). Other genes, with reduced expression, such as Notch3, are also of potential significance to HGPS, as mutations predispose patients to ischemic stroke (CADASIL) (Joutel et al., 1996).

## Defective ECM Synthesis Is Associated with a Reduction in Wnt-Mediated Lef1 Transcription

A question raised by these findings is how does a disrupted nuclear lamina result in alterations to cell membrane centered functions, specifically production of a functional ECM? Impairment of canonical Wnt signaling is an attractive explanation for

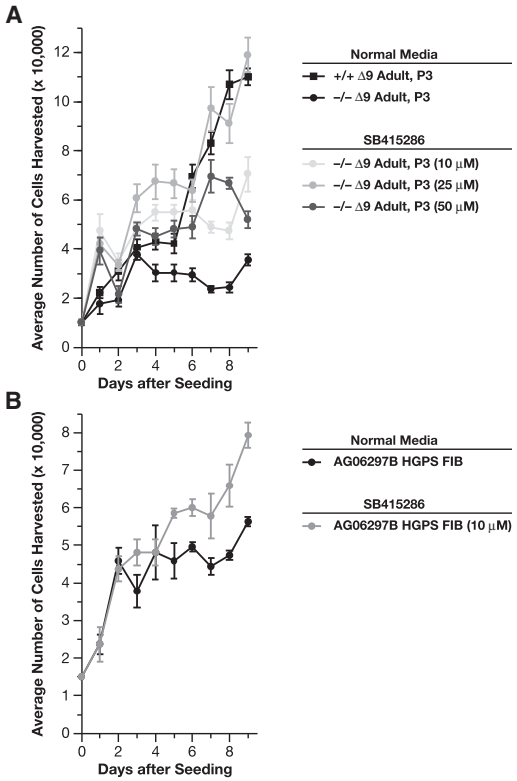


**Figure 7. Cell Proliferation Is Enhanced by Gsk-3β Inhibition**

(A) Treatment of Δ9MAFs with the Gsk inhibitor SB415286 (25 μm) rescues growth.

(B) Treatment of the progeric line AG06297 (10 μm SB415286) enhances growth.

Error bars are SEM.

the progeric phenotype, as central to this pathway is β-catenin which has dual functions in mediating cell-cell/matrix attachment and as a transcriptional cofactor (Behrens et al., 1996). Wnts regulate skeletogenesis and chondrogenesis (Chen et al., 2008; Day et al., 2005), ECM composition, fibronectin expression, and also inhibit proapoptotic gene expression in fibroblasts and osteoblasts (Almeida et al., 2005; Chen et al., 2007).

*Lmna*Δ9, and to a lesser extent Δ50, inhibit β-catenin transcriptional activity. The SSIM variants, which cannot be farnesylated, were less effective at inhibition. This indicates the deletions, as well as persistent farnesylation, of Δ9 and Δ50, contribute to transcriptional inhibition, consistent with mice expressing an unfarnesylated form of Δ50 developing a slightly milder pathology, compared with mice expressing the farnesylated form of Δ50 (Yang et al., 2008). β-catenin levels were unaffected; however, expression of Lef1 was greatly reduced. The reduction correlated with diminished Lef1 binding to the Col11a1 promoter, revealing a direct role of Lef1 in regulating the expression of at least some of the ECM genes in the Δ9MAFs.

The basis for how Δ9 and Δ50 affect the reduction in Lef1 levels remains obscure. A possibility is that nuclear import/retention of β-catenin is insufficient, because β-catenin regulates Lef1 expression (Hovanes et al., 2001). The *Xenopus* results indicate that the Nodal-Smad and Notch signaling pathways are intact and global nuclear transport appears to be unaffected. The translocation/retention of β-catenin and/or Lef1 into the nucleus may be specifically impaired, consistent with the reduced levels of β-catenin/Tcf/Lef complexes in the GST pull-down studies. Nuclear import and retention of β-catenin is complex, involving many factors (Willert and Jones, 2006). β-catenin does not have a nuclear localization sequence and nuclear import may be mediated by direct interactions with nuclear pore components, independent of the importin/karyopherin pathway (Fagotto et al., 1998). Progerin and Δ9 may interfere with nuclear import/export by potentially disrupting nuclear pore function, although it is not clear if progerin's effect on nuclear transport is specific or a consequence of generalized cell stress (S. Adam, personal communication). Significantly, only Lef1 expression, but not the related factors Tcf4 or 3, was reduced, suggesting that Lef1 may depend on some specific import/retention process differing from the other Tcfs. It is also noted that Lef1 is not expressed in +/+MEFs. MEFs may therefore differ from MAFs in their transcription factor requirements, and this may be a basis for the differences in the ECM/proliferation between Δ9MEFs and MAFs. Together, these results are consistent with earlier studies where heterozygous Lef1 mice show diminished bone mass and those null for Lef1 are postnatally growth retarded, have defective hair and tooth formation, tissues markedly affected in progeria (Noh et al., 2009; van Genderen et al., 1994). In addition, in *Zmpste24* null mice, where Lamin A remains farnesylated, Wnt signaling is reduced in hair follicles (Espada et al., 2008).

Besides Δ9 reducing Lef1 nuclear levels, Δ9 disrupts lamina and NE organization. Within the NE is the LINC complex, comprising KASH and SUN domain proteins, whose localization to the NE, in part, depends on the lamins (Crisp et al., 2006; Starr and Han, 2002). We now believe the nucleus does not float around the cytoplasm like some unruly zeppelin, and is instead physically tethered to the cytoskeleton by interactions between the LINC complex and the three components of the cytoskeleton (Crisp et al., 2006; Wilhelmsen et al., 2005). LINC disruption correlates with a reduction in cytoplasmic stiffness, probably due to changes in actin dynamics and/or organization and a reduction in RhoA activity (Hale et al., 2008; Lammerding et al., 2004). Such changes to cytoskeletal dynamics may affect the synthesis and organization of the ECM, as well as Wnt signaling, compounding the inhibition of Lef1 transcription (Chapados et al., 2006; Chen et al., 2006).

In conclusion, our data reveal that progeric mutations within the *LMNA* gene inhibit the Wnt pathway resulting in a reduction in LEF1 function and defective ECM synthesis. Our results provide support for the hypothesis, based on the few autopsies from progeric patients, that progeria is a disease of the ECM and connective tissue (Stehbens et al., 1999). This manifests by abnormalities in skeletal homeostasis, dentition, connective tissue, skin, and the vasculature (Merideth et al., 2008; Stehbens et al., 1999). If these failures are due to defective Wnt signaling and/or cytoskeletal-ECM function, then they suggest possible new routes of intervention, which may help in treating the disease. Finally, Wnt signaling and its role in aging and senescence has attracted significant attention (Manolagas and Almeida, 2007), although much of the evidence is seemingly contradictory (DeCarolis et al., 2008). What Progeria tells us

about the normal aging process is also controversial (Ershler et al., 2008). However, defective lamin processing may, at least, underlie the normal aging processes in the vascular system (Ragnauth et al., 2010).

## EXPERIMENTAL PROCEDURES

### Mouse Strains

The *Lmna*$^{L530P/L530P}$ (herein *Lmna*$^{\Delta 9/\Delta 9}$) mice are previously described (Mounkes et al., 2003). Care was provided in accordance to procedures in the Guide for the Care and Use of Laboratory Animals (NIH Publication No. 86-23, 1985).

### Plasmids and Antibodies

LMNAΔ50, LMNAΔ9, CSIM, and SSIM variants and LMNA tail (r390-664) were derived from HA- or Myc-tagged *LMNA* in pcDNA3.1 (Raharjo et al., 2001) by PCR mutagenesis. Retroviral expression vectors for the WT or mutant *LMNA* gene expression were derived from pBabe-puro. Vectors expressing GST, Cad-GST, and TCF-GST were a gift from Dr. Cara Gottardi. All antibodies used in this study are listed in Supplemental Experimental Procedures.

### Primary Cell Lines, Proliferation, and Apoptosis Assays

PMEFs and PMAFs were established as described (Mounkes et al., 2003). Cells were maintained in Dulbecco's MEM (Chemicon)+10% fetal calf serum (Invitrogen). Serum starvation medium contained 0.5% fetal calf serum.

#### *Proliferation Assays*

For single-passage short-term growth assays, cells were plated at $10^4$/well in 12-well dishes and counted daily, in triplicate. Continuous passage assays were performed according to the 3T3 protocol (Todaro and Green, 1963), beginning one passage after derivation.

#### *Apoptosis and TUNEL Assays*

Apoptosis and TUNEL assays were performed using the Vybrant Apoptosis Assay Kit #2 (Molecular Probes) and in situ cell death detection kit (Roche) according to the manufacturer's instructions. Cell sampling and data collection were by FACScan, B-D Immunocytometry Systems, and data analysis was performed with Analysis Modfit software (Verity).

### Transient Transfection and Luciferase Reporter Assays

HEK293 cells ($1 \times 10^5$) were cotransfected using Fugene 6 (Roche) with 2 mg of Renilla luciferase internal standard pRLCMV (Upstate Biotechnology), and/or 2 μg TOPFlash or FOPFlash firefly luciferase reporter plasmid (Promega) with 2 mg β-catenin (human full-length cDNA in pcDNA3.1) and/or with wild-type or lamin mutants (full-length cDNAs described above). pcDNA3.1 (Invitrogen) plasmid was added to equalize the amounts of DNA transfected. After 48 hr, luciferase activity was determined with the Dual-Luciferase assay system (Promega) as described by the manufacturer. The renilla luciferase vector, under control of a CMV promoter, was used to normalize transfection efficiencies.

### *Xenopus* Embryo Injections

PCR generated full-length mRNAs of the *LMNA* variants were cloned into the pCS+ vector. *Xenopus* embryos were microinjected with mRNA derived from *Not*I-linearized constructs transcribed with the mMessage mMachine kit (Ambion). *LMNA* RNAs (2.5 ng) were coinjected with 1.15 and 0.46 pg of *Xwnt3a* and *Xwnt8* RNA, respectively, into the two ventral blastomeres of four-cell stage embryos and the embryos cultured to the larval stage before scoring.

### In Vitro Translations

In vitro translations were performed as previously described (Crisp et al., 2006). To detect farnesylation, 9mCi $^3$H-mevalonolactone (American Radiolabeled Chemicals) was used in place of $^{35}$S-Translabel (MP Biolabs). The FTI PB-43 was a gift from M. Gelb.

### GST Pull-Down Assays

GST, cadherin-GST, or TCF–GST fusion proteins were expressed in *Escherichia coli* and purified using glutathione agarose beads as described (Gottardi and Gumbiner, 2004). GST fusion protein complexes were eluted from the beads and separated by SDS-PAGE, transferred to PVDF membranes, blotted with rabbit β-catenin antibody diluted 1:1000, and detected by chemiluminescence.

### Chromatin Immunoprecipitation Assay

Chromatin immunoprecipitation assay was performed according to the manufacturer's instructions using an EZ-Zyme Enzymatic Chromatin Prep Kit (Millipore).

### Microarray Analysis and Real-Time PCR

Total RNA was isolated from three independent triplicate cultures of wild-type and *Lmna*Δ9 MAFs at the similar confluencies, after 72 hr of serum starvation. Labeled samples were hybridized to Affymetrix Mouse Genome 430A 2.0 arrays. Data analysis was performed using the RMA normalization algorithm of BRB-Array Tools version 3.7 (Biometrics Research Branch, NCI; http://linus.nci.nih.gov/BRB-ArrayTools.html). Data sets containing significant genes deregulated in *Lmna*Δ9 were classified using Gene Ontology and DAVID bioinformatics resources (Huang da et al., 2009). PCR quantification of mRNA expression was performed using Applied Biosystems relative quantification (RQ) protocols according to the manufacturer's instructions. For detailed procedures see Supplemental Experimental Procedures.

### Microcomputed Tomography Scans

*Lmna*$^{+/+}$ and *Lmna*Δ9 mice were examined by compact cone-beam tomography (μCT40 scanner; Scanco Medical). Whole-body scans were performed as previously described (Yang et al., 2008). μCT analysis of the axial and limb bones was performed as previously described (Sawyer et al., 2009) except scanning width was at 35 mm and CTan software used for the calculations. See Supplemental Experimental Procedures.

## ACCESSION NUMBERS

The data are deposited in NCBI's Gene Expression Omnibus and are accessible through GEO Series accession number GSE23495 (http://www.ncbi.nlm.nih.gov/geo/query/acc.cgi?acc = GSE23495).

## SUPPLEMENTAL INFORMATION

Supplemental Information includes three figures and two tables and can be found with this article online at doi:10.1016/j.devcel.2010.08.013.

## ACKNOWLEDGMENTS

We thank T. Yamaguchi, J. Pollard, and J. Campisi for advice, C. B. DeMille for guidance, M. Gelb for PB-43, R. Frederickson, A. Kane for producing the figures, K. Rogers for histology, and anonymous reviewers for helpful suggestions. These studies were funded in part by the Center for Cancer Research, NCI, and NIH and NIH Grant R01HD057873 to J.-W.J. We report no conflict of interest.

Received: July 27, 2009
Revised: July 7, 2010
Accepted: August 23, 2010
Published: September 13, 2010

## REFERENCES

Adams, J.C., and Watt, F.M. (1993). Regulation of development and differentiation by the extracellular matrix. Development *117*, 1183–1198.

Almeida, M., Han, L., Bellido, T., Manolagas, S.C., and Kousteni, S. (2005). Wnt proteins prevent apoptosis of both uncommitted osteoblast progenitors and differentiated osteoblasts by beta-catenin-dependent and -independent signaling cascades involving Src/ERK and phosphatidylinositol 3-kinase/AKT. J. Biol. Chem. *280*, 41342–41351.

Ameye, L., and Young, M.F. (2002). Mice deficient in small leucine-rich proteoglycans: novel in vivo models for osteoporosis, osteoarthritis, Ehlers-Danlos

syndrome, muscular dystrophy, and corneal diseases. Glycobiology *12*, 107R–116R.

Aszodi, A., Legate, K.R., Nakchbandi, I., and Fassler, R. (2006). What mouse mutants teach us about extracellular matrix function. Annu. Rev. Cell Dev. Biol. *22*, 591–621.

Behrens, J., von Kries, J.P., Kuhl, M., Bruhn, L., Wedlich, D., Grosschedl, R., and Birchmeier, W. (1996). Functional interaction of beta-catenin with the transcription factor LEF-1. Nature *382*, 638–642.

Bergo, M.O., Gavino, B., Ross, J., Schmidt, W.K., Hong, C., Kendall, L.V., Mohr, A., Meta, M., Genant, H., Jiang, Y., et al. (2002). Zmpste24 deficiency in mice causes spontaneous bone fractures, muscle weakness, and a prelamin A processing defect. Proc. Natl. Acad. Sci. USA *99*, 13049–13054.

Bridger, J.M., and Kill, I.R. (2004). Aging of Hutchinson-Gilford progeria syndrome fibroblasts is characterised by hyperproliferation and increased apoptosis. Exp. Gerontol. *39*, 717–724.

Brink, H.E., Stalling, S.S., and Nicoll, S.B. (2005). Influence of serum on adult and fetal dermal fibroblast migration, adhesion, and collagen expression. In Vitro Cell. Dev. Biol. Anim. *41*, 252–257.

Brooke, B.S., Karnik, S.K., and Li, D.Y. (2003). Extracellular matrix in vascular morphogenesis and disease: structure versus signal. Trends Cell Biol. *13*, 51–56.

Burke, B., and Stewart, C.L. (2006). The laminopathies: the functional architecture of the nucleus and its contribution to disease (*). Annu. Rev. Genomics Hum. Genet. *7*, 369–405.

Capell, B.C., Erdos, M.R., Madigan, J.P., Fiordalisi, J.J., Varga, R., Conneely, K.N., Gordon, L.B., Der, C.J., Cox, A.D., and Collins, F.S. (2005). Inhibiting farnesylation of progerin prevents the characteristic nuclear blebbing of Hutchinson-Gilford progeria syndrome. Proc. Natl. Acad. Sci. USA *102*, 12879–12884.

Chang, H.Y., Chi, J.T., Dudoit, S., Bondre, C., van de Rijn, M., Botstein, D., and Brown, P.O. (2002). Diversity, topographic differentiation, and positional memory in human fibroblasts. Proc. Natl. Acad. Sci. USA *99*, 12877–12882.

Chapados, R., Abe, K., Ihida-Stansbury, K., McKean, D., Gates, A.T., Kern, M., Merklinger, S., Elliott, J., Plant, A., Shimokawa, H., et al. (2006). ROCK controls matrix synthesis in vascular smooth muscle cells: coupling vasoconstriction to vascular remodeling. Circ. Res. *99*, 837–844.

Chen, H.J., Lin, C.M., Lin, C.S., Perez-Olle, R., Leung, C.L., and Liem, R.K. (2006). The role of microtubule actin cross-linking factor 1 (MACF1) in the Wnt signaling pathway. Genes Dev. *20*, 1933–1945.

Chen, S., McLean, S., Carter, D.E., and Leask, A. (2007). The gene expression profile induced by Wnt 3a in NIH 3T3 fibroblasts. J Cell Commun Signal *1*, 175–183.

Chen, M., Zhu, M., Awad, H., Li, T.F., Sheu, T.J., Boyce, B.F., Chen, D., and O'Keefe, R.J. (2008). Inhibition of beta-catenin signaling causes defects in postnatal cartilage development. J. Cell Sci. *121*, 1455–1465.

Coghlan, M.P., Culbert, A.A., Cross, D.A., Corcoran, S.L., Yates, J.W., Pearce, N.J., Rausch, O.L., Murphy, G.J., Carter, P.S., Roxbee Cox, L., et al. (2000). Selective small molecule inhibitors of glycogen synthase kinase-3 modulate glycogen metabolism and gene transcription. Chem. Biol. *7*, 793–803.

Corrigan, D.P., Kuszczak, D., Rusinol, A.E., Thewke, D.P., Hrycyna, C.A., Michaelis, S., and Sinensky, M.S. (2005). Prelamin A endoproteolytic processing in vitro by recombinant Zmpste24. Biochem. J. *387*, 129–138.

Corsi, A., Xu, T., Chen, X.D., Boyde, A., Liang, J., Mankani, M., Sommer, B., Iozzo, R.V., Eichstetter, I., Robey, P.G., et al. (2002). Phenotypic effects of biglycan deficiency are linked to collagen fibril abnormalities, are synergized by decorin deficiency, and mimic Ehlers-Danlos-like changes in bone and other connective tissues. J. Bone Miner. Res. *17*, 1180–1189.

Crisp, M., Liu, Q., Roux, K., Rattner, J.B., Shanahan, C., Burke, B., Stahl, P.D., and Hodzic, D. (2006). Coupling of the nucleus and cytoplasm: role of the LINC complex. J. Cell Biol. *172*, 41–53.

Csoka, A.B., Cao, H., Sammak, P.J., Constantinescu, D., Schatten, G.P., and Hegele, R.A. (2004a). Novel lamin A/C gene (LMNA) mutations in atypical progeroid syndromes. J. Med. Genet. *41*, 304–308.

Csoka, A.B., English, S.B., Simkevich, C.P., Ginzinger, D.G., Butte, A.J., Schatten, G.P., Rothman, F.G., and Sedivy, J.M. (2004b). Genome-scale expression profiling of Hutchinson-Gilford progeria syndrome reveals widespread transcriptional misregulation leading to mesodermal/mesenchymal defects and accelerated atherosclerosis. Aging Cell *3*, 235–243.

Day, T.F., Guo, X., Garrett-Beal, L., and Yang, Y. (2005). Wnt/beta-catenin signaling in mesenchymal progenitors controls osteoblast and chondrocyte differentiation during vertebrate skeletogenesis. Dev. Cell *8*, 739–750.

De Sandre-Giovannoli, A., Bernard, R., Cau, P., Navarro, C., Amiel, J., Boccaccio, I., Lyonnet, S., Stewart, C.L., Munnich, A., Le Merrer, M., et al. (2003). Lamin a truncation in Hutchinson-Gilford progeria. Science *300*, 2055.

DeCarolis, N.A., Wharton, K.A., Jr., and Eisch, A.J. (2008). Which way does the Wnt blow? Exploring the duality of canonical Wnt signaling on cellular aging. Bioessays *30*, 102–106.

Dechat, T., Shimi, T., Adam, S.A., Rusinol, A.E., Andres, D.A., Spielmann, H.P., Sinensky, M.S., and Goldman, R.D. (2007). Alterations in mitosis and cell cycle progression caused by a mutant lamin A known to accelerate human aging. Proc. Natl. Acad. Sci. USA *104*, 4955–4960.

Ellis, I.R., and Schor, S.L. (1996). Differential effects of TGF-beta1 on hyaluronan synthesis by fetal and adult skin fibroblasts: implications for cell migration and wound healing. Exp. Cell Res. *228*, 326–333.

Eriksson, M., Brown, W.T., Gordon, L.B., Glynn, M.W., Singer, J., Scott, L., Erdos, M.R., Robbins, C.M., Moses, T.Y., Berglund, P., et al. (2003). Recurrent de novo point mutations in lamin A cause Hutchinson-Gilford progeria syndrome. Nature *423*, 293–298.

Ershler, W.B., Ferrucci, L., and Longo, D.L. (2008). Hutchinson-Gilford progeria syndrome. N. Engl. J. Med. *358*, 2409–2410.

Espada, J., Varela, I., Flores, I., Ugalde, A.P., Cadinanos, J., Pendas, A.M., Stewart, C.L., Tryggvason, K., Blasco, M.A., Freije, J.M., et al. (2008). Nuclear envelope defects cause stem cell dysfunction in premature-aging mice. J. Cell Biol. *181*, 27–35.

Fagotto, F., Gluck, U., and Gumbiner, B.M. (1998). Nuclear localization signal-independent and importin/karyopherin-independent nuclear import of beta-catenin. Curr. Biol. *8*, 181–190.

Friedman, D.B., and Johnson, T.E. (1988). A mutation in the age-1 gene in Caenorhabditis elegans lengthens life and reduces hermaphrodite fertility. Genetics *118*, 75–86.

Gerace, L., and Burke, B. (1988). Functional organization of the nuclear envelope. Annu. Rev. Cell Biol. *4*, 335–374.

Gilford, H. (1904). Ateleiosis and progeria. BMJ *2*, 914–918.

Glynn, M.W., and Glover, T.W. (2005). Incomplete processing of mutant lamin A in Hutchinson-Gilford progeria leads to nuclear abnormalities, which are reversed by farnesyltransferase inhibition. Hum. Mol. Genet. *14*, 2959–2969.

Goldman, R.D., Shumaker, D.K., Erdos, M.R., Eriksson, M., Goldman, A.E., Gordon, L.B., Gruenbaum, Y., Khuon, S., Mendez, M., Varga, R., et al. (2004). Accumulation of mutant lamin A causes progressive changes in nuclear architecture in Hutchinson-Gilford progeria syndrome. Proc. Natl. Acad. Sci. USA *101*, 8963–8968.

Gospodarowicz, D., Delgado, D., and Vlodavsky, I. (1980). Permissive effect of the extracellular matrix on cell proliferation in vitro. Proc. Natl. Acad. Sci. USA *77*, 4094–4098.

Gottardi, C.J., and Gumbiner, B.M. (2004). Distinct molecular forms of beta-catenin are targeted to adhesive or transcriptional complexes. J. Cell Biol. *167*, 339–349.

Hale, C.M., Shrestha, A.L., Khatau, S.B., Stewart-Hutchinson, P.J., Hernandez, L., Stewart, C.L., Hodzic, D., and Wirtz, D. (2008). Dysfunctional connections between the nucleus and the actin and microtubule networks in laminopathic models. Biophys. J. *95*, 5462–5475.

Hennekes, H., and Nigg, E.A. (1994). The role of isoprenylation in membrane attachment of nuclear lamins. A single point mutation prevents proteolytic cleavage of the lamin A precursor and confers membrane binding properties. J. Cell Sci. *107*, 1019–1029.

Hovanes, K., Li, T.W., Munguia, J.E., Truong, T., Milovanovic, T., Lawrence Marsh, J., Holcombe, R.F., and Waterman, M.L. (2001). Beta-catenin-sensitive isoforms of lymphoid enhancer factor-1 are selectively expressed in colon cancer. Nat. Genet. *28*, 53–57.

Huang da, W., Sherman, B.T., and Lempicki, R.A. (2009). Systematic and integrative analysis of large gene lists using DAVID bioinformatics resources. Nat. Protoc. *4*, 44–57.

Hutchinson, J. (1886). Congenital absence of hair and mammary glands with atrophic condition of the skin and its appendages. Transactions of the Medico-Chirurgical Society of Edinburgh *69*, 473–477.

Irizarry, R.A., Bolstad, B.M., Collin, F., Cope, L.M., Hobbs, B., and Speed, T.P. (2003). Summaries of Affymetrix GeneChip probe level data. Nucleic Acids Res. *31*, e15.

Jones, C.M., Kuehn, M.R., Hogan, B.L., Smith, J.C., and Wright, C.V. (1995). Nodal-related signals induce axial mesoderm and dorsalize mesoderm during gastrulation. Development *121*, 3651–3662.

Joutel, A., Corpechot, C., Ducros, A., Vahedi, K., Chabriat, H., Mouton, P., Alamowitch, S., Domenga, V., Cecillion, M., Marechal, E., et al. (1996). Notch3 mutations in CADASIL, a hereditary adult-onset condition causing stroke and dementia. Nature *383*, 707–710.

Kadler, K.E., Hill, A., and Canty-Laird, E.G. (2008). Collagen fibrillogenesis: fibronectin, integrins, and minor collagens as organizers and nucleators. Curr. Opin. Cell Biol. *20*, 495–501.

Kahler, R.A., Yingst, S.M., Hoeppner, L.H., Jensen, E.D., Krawczak, D., Oxford, J.T., and Westendorf, J.J. (2008). Collagen 11a1 is indirectly activated by lymphocyte enhancer-binding factor 1 (Lef1) and negatively regulates osteoblast maturation. Matrix Biol. *27*, 330–338.

Kennedy, B.K., Austriaco, N.R., Jr., Zhang, J., and Guarente, L. (1995). Mutation in the silencing gene SIR4 can delay aging in S. cerevisiae. Cell *80*, 485–496.

Kjaer, M. (2004). Role of extracellular matrix in adaptation of tendon and skeletal muscle to mechanical loading. Physiol. Rev. *84*, 649–698.

Lammerding, J., Schulze, P.C., Takahashi, T., Kozlov, S., Sullivan, T., Kamm, R.D., Stewart, C.L., and Lee, R.T. (2004). Lamin A/C deficiency causes defective nuclear mechanics and mechanotransduction. J. Clin. Invest. *113*, 370–378.

Liu, B., Wang, J., Chan, K.M., Tjia, W.M., Deng, W., Guan, X., Huang, J.D., Li, K.M., Chau, P.Y., Chen, D.J., et al. (2005). Genomic instability in laminopathy-based premature aging. Nat. Med. *11*, 780–785.

Liu, Y., Rusinol, A., Sinensky, M., Wang, Y., and Zou, Y. (2006). DNA damage responses in progeroid syndromes arise from defective maturation of prelamin A. J. Cell Sci. *119*, 4644–4649.

Lutz, R.J., Trujillo, M.A., Denham, K.S., Wenger, L., and Sinensky, M. (1992). Nucleoplasmic localization of prelamin A: implications for prenylation-dependent lamin A assembly into the nuclear lamina. Proc. Natl. Acad. Sci. USA *89*, 3000–3004.

Manolagas, S.C., and Almeida, M. (2007). Gone with the Wnts: beta-catenin, T-cell factor, forkhead box O, and oxidative stress in age-dependent diseases of bone, lipid, and glucose metabolism. Mol. Endocrinol. *21*, 2605–2614.

McClintock, D., Gordon, L.B., and Djabali, K. (2006). Hutchinson-Gilford progeria mutant lamin A primarily targets human vascular cells as detected by an anti-Lamin A G608G antibody. Proc. Natl. Acad. Sci. USA *103*, 2154–2159.

McClintock, D., Ratner, D., Lokuge, M., Owens, D.M., Gordon, L.B., Collins, F.S., and Djabali, K. (2007). The mutant form of lamin A that causes Hutchinson-Gilford progeria is a biomarker of cellular aging in human skin. PLoS One *2*, e1269.

Merideth, M.A., Gordon, L.B., Clauss, S., Sachdev, V., Smith, A.C., Perry, M.B., Brewer, C.C., Zalewski, C., Kim, H.J., Solomon, B., et al. (2008). Phenotype and course of Hutchinson-Gilford progeria syndrome. N. Engl. J. Med. *358*, 592–604.

Morin, P.J., Sparks, A.B., Korinek, V., Barker, N., Clevers, H., Vogelstein, B., and Kinzler, K.W. (1997). Activation of beta-catenin-Tcf signaling in colon cancer by mutations in beta-catenin or APC. Science *275*, 1787–1790.

Mounkes, L.C., Kozlov, S., Hernandez, L., Sullivan, T., and Stewart, C.L. (2003). A progeroid syndrome in mice is caused by defects in A-type lamins. Nature *423*, 298–301.

Noh, T., Gabet, Y., Cogan, J., Shi, Y., Tank, A., Sasaki, T., Criswell, B., Dixon, A., Lee, C., Tam, J., et al. (2009). Lef1 haploinsufficient mice display a low turnover and low bone mass phenotype in a gender- and age-specific manner. PLoS ONE *4*, e5438.

Ragnauth, C.D., Warren, D.T., Liu, Y., McNair, R., Tajsic, T., Figg, N., Shroff, R., Skepper, J., and Shanahan, C.M. (2010). Prelamin A acts to accelerate smooth muscle cell senescence and is a novel biomarker of human vascular aging. Circulation *121*, 2200–2210.

Raharjo, W.H., Enarson, P., Sullivan, T., Stewart, C.L., and Burke, B. (2001). Nuclear envelope defects associated with LMNA mutations cause dilated cardiomyopathy and Emery-Dreifuss muscular dystrophy. J. Cell Sci. *114*, 4447–4457.

Rober, R.A., Weber, K., and Osborn, M. (1989). Differential timing of nuclear lamin A/C expression in the various organs of the mouse embryo and the young animal: a developmental study. Development *105*, 365–378.

Rodriguez, S., Coppede, F., Sagelius, H., and Eriksson, M. (2009). Increased expression of the Hutchinson-Gilford progeria syndrome truncated lamin A transcript during cell aging. Eur. J. Hum. Genet. *17*, 928–937.

Sawyer, A.A., Song, S.J., Susanto, E., Chuan, P., Lam, C.X., Woodruff, M.A., Hutmacher, D.W., and Cool, S.M. (2009). The stimulation of healing within a rat calvarial defect by mPCL-TCP/collagen scaffolds loaded with rhBMP-2. Biomaterials *30*, 2479–2488.

Scaffidi, P., and Misteli, T. (2005). Reversal of the cellular phenotype in the premature aging disease Hutchinson-Gilford progeria syndrome. Nat. Med. *11*, 440–445.

Scaffidi, P., and Misteli, T. (2006). Lamin A-dependent nuclear defects in human aging. Science *312*, 1059–1063.

Scaffidi, P., and Misteli, T. (2008). Lamin A-dependent misregulation of adult stem cells associated with accelerated ageing. Nat. Cell Biol. *10*, 452–459.

Starr, D.A., and Han, M. (2002). Role of ANC-1 in tethering nuclei to the actin cytoskeleton. Science *298*, 406–409.

Stehbens, W.E., Wakefield, S.J., Gilbert-Barness, E., Olson, R.E., and Ackerman, J. (1999). Histological and ultrastructural features of atherosclerosis in progeria. Cardiovasc. Pathol. *8*, 29–39.

Stehbens, W.E., Delahunt, B., Shozawa, T., and Gilbert-Barness, E. (2001). Smooth muscle cell depletion and collagen types in progeric arteries. Cardiovasc. Pathol. *10*, 133–136.

Stewart, C., and Burke, B. (1987). Teratocarcinoma stem cells and early mouse embryos contain only a single major lamin polypeptide closely resembling lamin B. Cell *51*, 383–392.

Sullivan, T., Escalante-Alcalde, D., Bhatt, H., Anver, M., Bhat, N., Nagashima, K., Stewart, C.L., and Burke, B. (1999). Loss of A-type lamin expression compromises nuclear envelope integrity leading to muscular dystrophy. J. Cell Biol. *147*, 913–920.

Thomas, P.D., Campbell, M.J., Kejariwal, A., Mi, H., Karlak, B., Daverman, R., Diemer, K., Muruganujan, A., and Narechania, A. (2003). PANTHER: a library of protein families and subfamilies indexed by function. Genome Res. *13*, 2129–2141.

Todaro, G.J., and Green, H. (1963). Quantitative studies of the growth of mouse embryo cells in culture and their development into established lines. J. Cell Biol. *17*, 299–313.

Toth, J.I., Yang, S.H., Qiao, X., Beigneux, A.P., Gelb, M.H., Moulson, C.L., Miner, J.H., Young, S.G., and Fong, L.G. (2005). Blocking protein farnesyltransferase improves nuclear shape in fibroblasts from humans with progeroid syndromes. Proc. Natl. Acad. Sci. USA *102*, 12873–12878.

van Genderen, C., Okamura, R.M., Farinas, I., Quo, R.G., Parslow, T.G., Bruhn, L., and Grosschedl, R. (1994). Development of several organs that require inductive epithelial-mesenchymal interactions is impaired in LEF-1-deficient mice. Genes Dev. *8*, 2691–2703.

Varela, I., Cadinanos, J., Pendas, A.M., Gutierrez-Fernandez, A., Folgueras, A.R., Sanchez, L.M., Zhou, Z., Rodriguez, F.J., Stewart, C.L., Vega, J.A., et al. (2005). Accelerated ageing in mice deficient in Zmpste24 protease is linked to p53 signalling activation. Nature *437*, 564–568.

Vernon, A.E., Movassagh, M., Horan, I., Wise, H., Ohnuma, S., and Philpott, A. (2006). Notch targets the Cdk inhibitor Xic1 to regulate differentiation but not the cell cycle in neurons. EMBO Rep. *7*, 643–648.

Wagenseil, J.E., and Mecham, R.P. (2009). Vascular extracellular matrix and arterial mechanics. Physiol. Rev. *89*, 957–989.

Wilhelmsen, K., Litjens, S.H., Kuikman, I., Tshimbalanga, N., Janssen, H., van den Bout, I., Raymond, K., and Sonnenberg, A. (2005). Nesprin-3, a novel outer nuclear membrane protein, associates with the cytoskeletal linker protein plectin. J. Cell Biol. *171*, 799–810.

Willert, K., and Jones, K.A. (2006). Wnt signaling: is the party in the nucleus? Genes Dev. *20*, 1394–1404.

Yang, S.H., Andres, D.A., Spielmann, H.P., Young, S.G., and Fong, L.G. (2008). Progerin elicits disease phenotypes of progeria in mice whether or not it is farnesylated. J. Clin. Invest. *118*, 3291–3300.

Yin, W., Xiang, P., and Li, Q. (2005). Investigations of the effect of DNA size in transient transfection assay using dual luciferase system. Anal. Biochem. *346*, 289–294.